

Figure 1(a) X-ray diffraction pattern and **(b)** EDX analysis of as-synthesized $\text{TiO}_2/\text{GO}/\text{CuFe}_2\text{O}_4$ nanocomposite

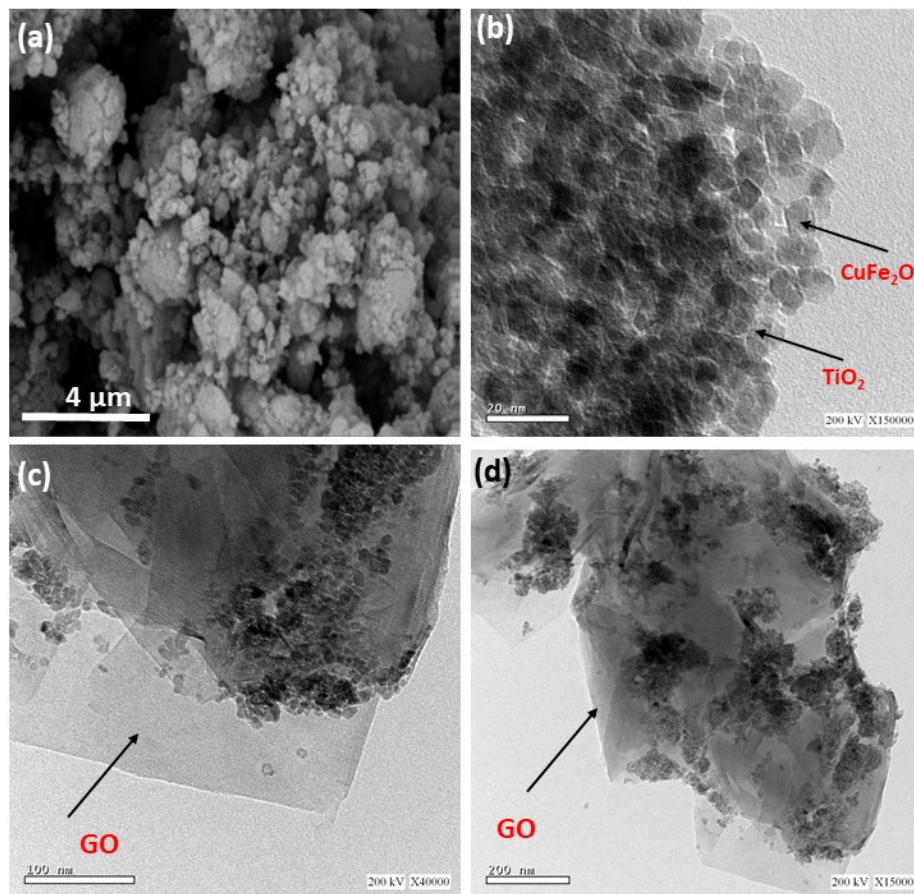


Figure 2(a) SEM and (b-d) TEM images of as-synthesized $\text{TiO}_2/\text{GO}/\text{CuFe}_2\text{O}_4$ nanocomposite

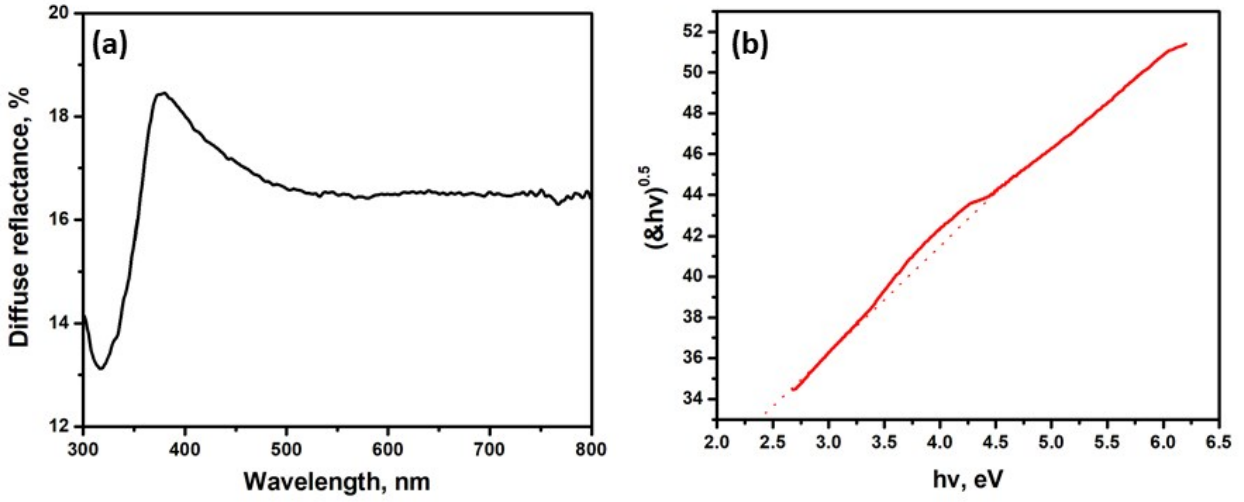


Figure 3(a) Diffused reflectance spectra and **(b)** Tauc plot of $\text{TiO}_2/\text{GO}/\text{CuFe}_2\text{O}_4$ nanocomposite

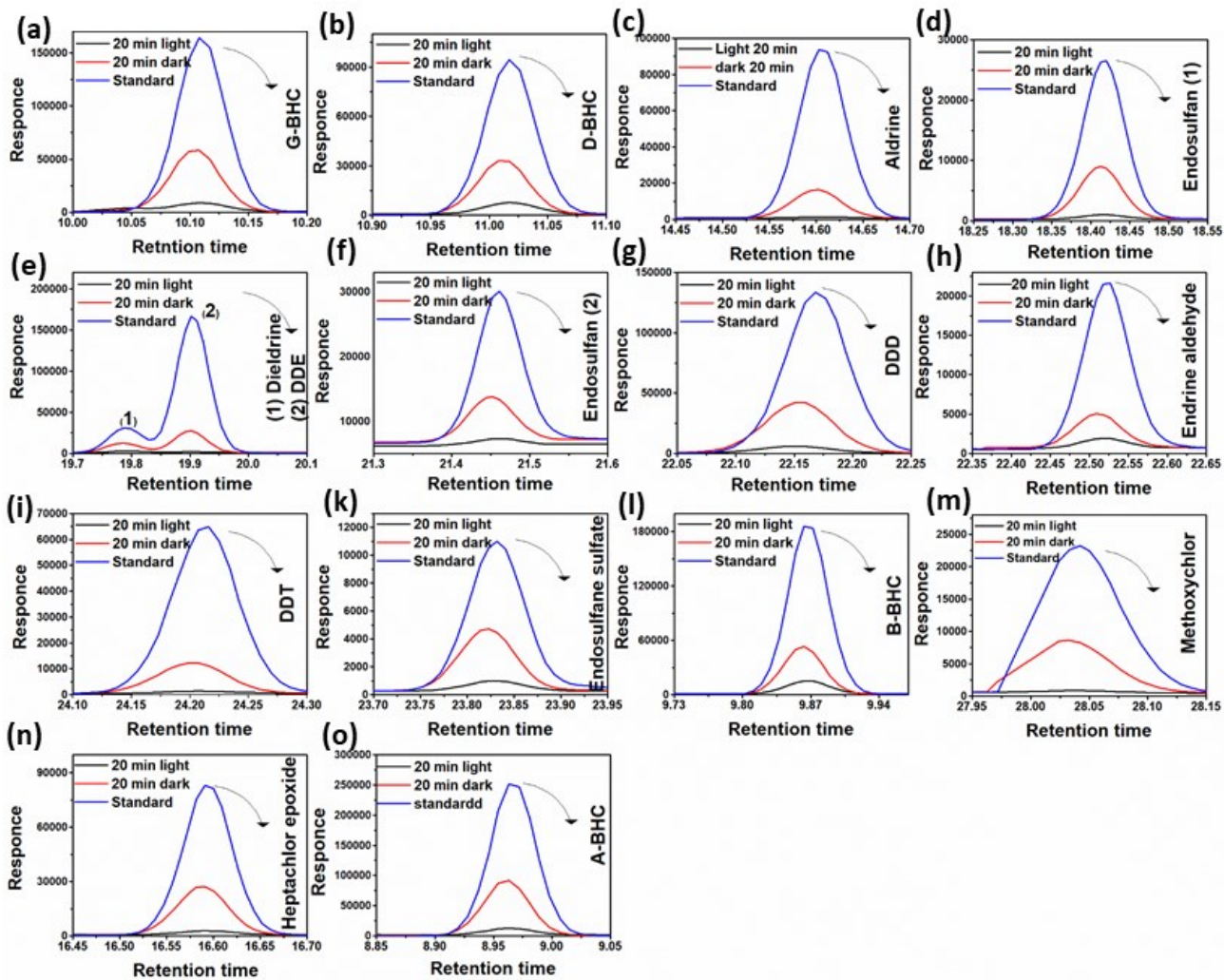


Figure 4(a-o) Peak elution change of selected pesticides vs retention times' using $\text{TiO}_2/\text{GO}/\text{CuFe}_2\text{O}_4$ nanocomposite

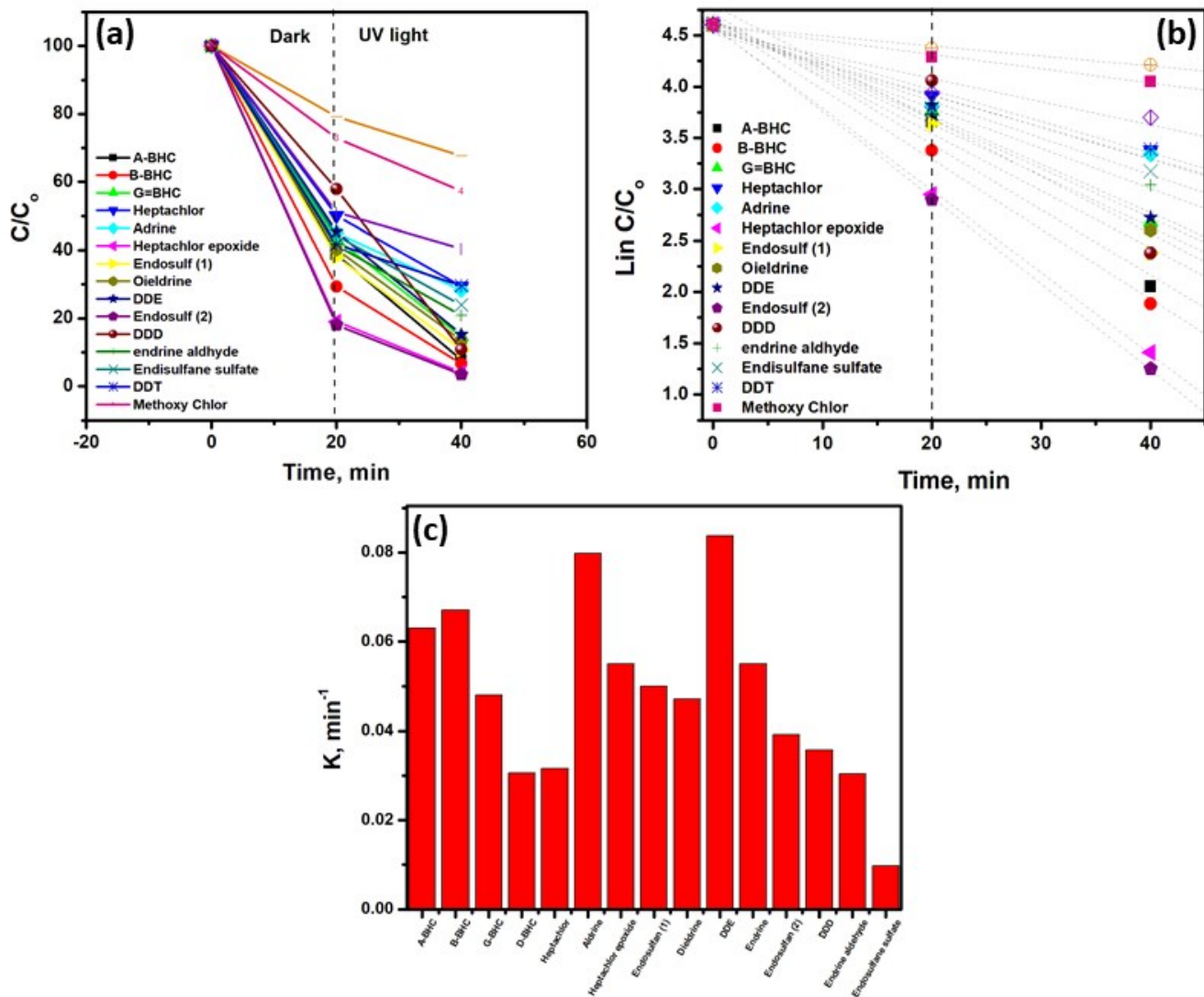


Figure 5 (a) Removal efficiency of selected pesticides as function of irradiation time, (b) $\ln(C/C_0)$ vs. time (min) curve for photodegradation of selected pesticides and (c) photodegradation rate in the presence of $\text{TiO}_2/\text{GO}/\text{CuFe}_2\text{O}_4$ nanocomposite

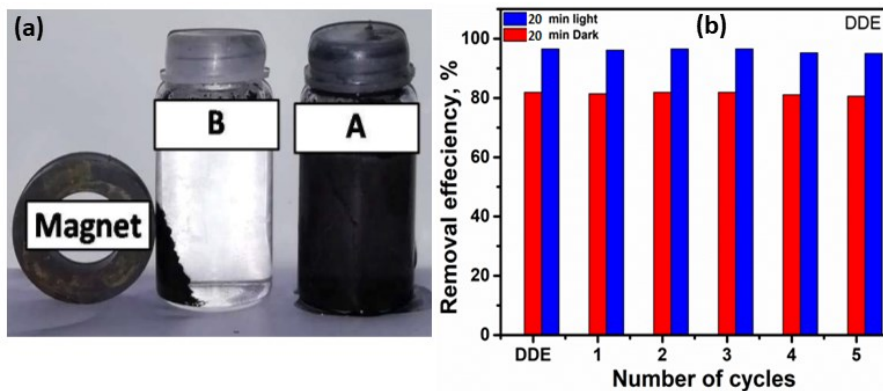


Figure 6 (a) Photograph of the magnetic nanocomposite solution, (b) the recyclability of DDE type of pesticide by $\text{TiO}_2/\text{GO}/\text{CuFe}_2\text{O}_4$ nanocomposite

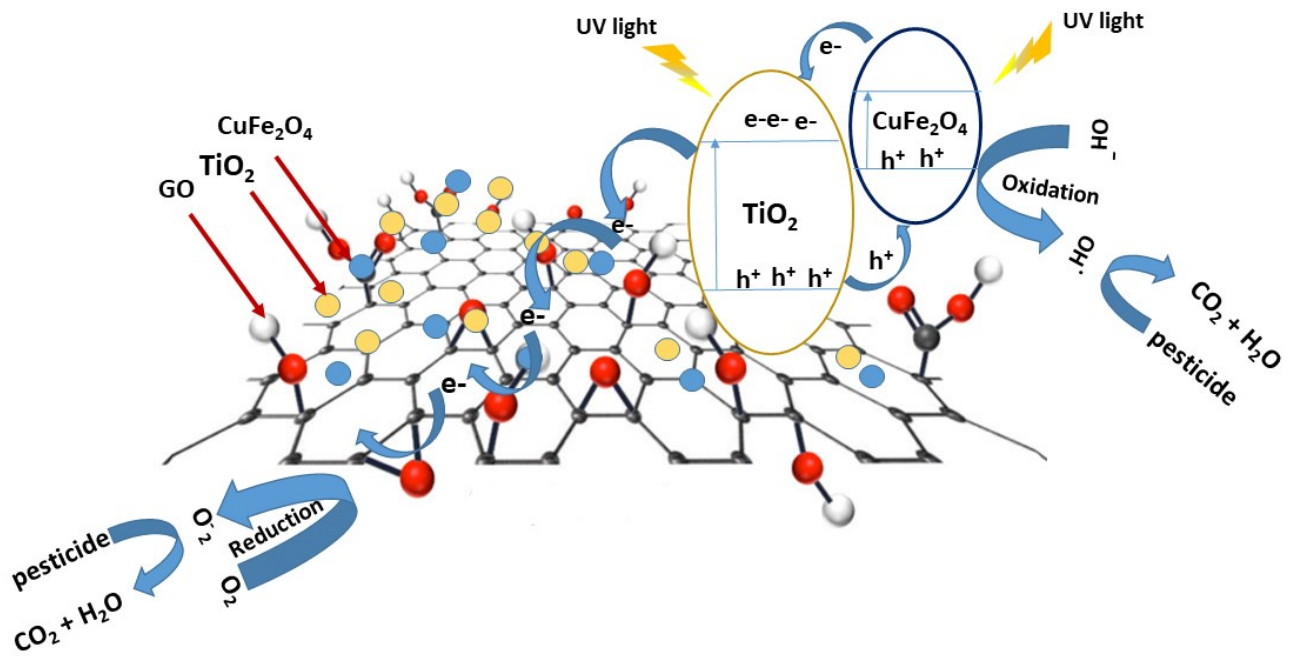


Figure 7 Proposed mechanisms of charge separation via direct Z-type scheme under UV illumination